Journal of Cellular Biochemistry

Ivermectin inhibits the growth of glioma cells by inducing cell cycle arrest and apoptosis in vitro and in vivo

Journal:	*Journal of Cellular Biochemistry*
Manuscript ID	Draft
Wiley - Manuscript type:	Research Article
Date Submitted by the Author:	n/a
Complete List of Authors:	Song, Dandan; Northeast Agricultural University, School of Life Science Liang, Hongsheng; Key Laboratory of Neurosurgery, College of Heilongjiang Province; The First Affiliated Hospital of Harbin Medical University, Harbin, China, Neurosurgery Qu, Bo; Northeast Agricultural University, School of Life Science Li, Yijing; Northeast Agricultural University, College of Veterinary Medicine Liu, Jingjing; Northeast Agricultural University, School of Life Science Zhang, Yanan; Northeast Agricultural University, School of Life Science Li, Lu; Northeast Agricultural University, School of Life Science Hu, Li; Key Laboratory of Neurosurgery, College of Heilongjiang Province; The First Affiliated Hospital of Harbin Medical University, Harbin, China, Neurosurgery Zhang, Xiangtong; Key Laboratory of Neurosurgery, College of Heilongjiang Province; The First Affiliated Hospital of Harbin Medical University, Harbin, China, Neurosurgery Gao, Aili; Northeast Agricultural University, School of Life Science
Keywords:	ivermectin, glioma, proliferation, apoptosis, cell cycle arrest

Title: Ivermectin inhibits the growth of glioma cells by inducing cell cycle arrest and apoptosis *in vitro* and *in vivo*

Authors: Dandan Song [a#], Hongsheng Liang[b#], Bo Qu [a], Yijing Li[c], Jingjing Liu [a], Yanan Zhang [a], Lu Li [a], Li Hu[b], Xiangtong Zhang[b], Aili Gao [a]*

[a] School of Life Science, Northeast Agricultural University, Harbin, China; [b] Key Laboratory of Neurosurgery, College of Heilongjiang Province; The First Affiliated Hospital of Harbin Medical University, Harbin, China; [c] College of Veterinary Medicine, Northeast Agricultural University, Harbin, China.

[#]Authors **Dandan Song** and **Hongsheng Liang** contributed equally to this work.

***Corresponding author:** Aili Gao

Address: School of Life Science, Northeast Agricultural University, 600 Changjiang Road, Xiangfang District, Harbin, 150030, P. R. China

Tel: 86-131-9950-0261

Fax: 86-451-5519-0413

Email: gaoaili2004@163.com

Abstract

Glioma, the most predominant primary malignant brain tumor, remains uncured due to the absence of effective treatments. Hence, it is imperative to develop successful therapeutic agents. This study aimed to explore the anti-tumor effects and mechanisms of ivermectin (IVM) in glioma cells *in vitro* and *in vivo*. The effects of IVM on cell viability, cell cycle arrest, apoptosis rate and morphologic characteristics were determined respectively by MTT assay/colony formation assay, flow cytometry and transmission electron microscope. Additionally, the expression levels of cycle-related and apoptosis-associated proteins were individually examined by western blotting. Moreover, cell proliferation and apoptosis analyses were carried out by TUNEL, Ki-67, Cleaved caspase-3 and Cleaved caspase-9 immunostaining assay. Our results demonstrated that IVM has a potential dosage-dependent inhibition effect on the apoptosis rate of glioma cells. Meanwhile, the results also revealed that IVM induced apoptosis by increasing caspase-3 and caspase-9 activity, up-regulating the expression of Bax, down-regulating Bcl-2, activating Cleaved caspase-3 and Cleaved caspase-9, and blocking cell cycle in G0/G1 phase by down-regulating levels of CDK2, CDK4, CDK6, Cyclin D1 and Cyclin E. These findings suggest that IVM has an inhibition effect on the proliferation of glioma cells by triggering cell cycle arrest and inducing cell apoptosis *in vitro* and *in vivo*, and probably represents promising agent for treating glioma.

Key words: ivermectin; glioma; proliferation; apoptosis; cell cycle arrest

Introduction

Glioma, short for neurogioma, is one of the most primary intracranial neoplasms, highly resistant to current therapy, and accounts for 33%-58% of all brain tumors [1, 2]. At present, therapy mainly consists of tumour excision by surgery, auxiliary assisted chemotherapy, immunotherapy and/or biological treatment in combination with chemotherapeutics like temozolomide (TMZ) to delay tumor recurrence and prolong patient survival [3-6]. Although the use of TMZ approved by the Food and Drug Administration (FDA) in 2005, it's administration is hampered by the high-dose regimen required to reach a suitable effective concentration in the target tissues, which provoking extensive toxic effects without increasing the risk/benefit ratio [7, 8].What's more, there is evidence indicated that dopamine has potential as a novel therapy for human malignant glioma but currently cannot be used as such because of its toxicity [9].Therefore, it is particularly important to develop more effective agents to treat glioma.

Recently, some macrocyclic lactones have been discovered to be effective for inhibiting proliferation of tumor cells [10, 11]. The macrocyclic lactones with lower toxicity are the most powerful agents and are used widely for fighting against ecto- and endoparasites in livestock, pets and humans [12]. Among these drugs, ivermectin (IVM), a broad-spectrum antiparasitic drug, is a dehydrated derivative of avermectin B1 and belongs to the avermectin family. The fact proved that IVM has increasing application in the treatment of river blindness, elephantiasis and various parasites [13]. Moreover, some studies demonstrate that IVM has obvious anti-proliferative activity in colon, ovarian, melanoma, leukemia and breast cancer cells by inducing apoptosis, suppressing initiation and malignant growth of cancer, activating necrosis pathways, reversing multidrug resistance, and blocking cell cycle progression, respectively [14-18]. In our previous work, we proved that macrocyclic lactones including

IVM could serve as potential effective MDR reversal agents. We also found that IVM was partially effective in killing non drug resistant tumor cells [19]. Recently, it was reported that the anticancer activity of IVM is mediated by affecting mitochondrial function and inducing oxidative stress to inhibit angiogenesis of glioblastoma [20], and that it could inhibit the pri-to-pre-miR-21 processing activity of DDX23 and decrease glioma cell proliferation [21]. However, the molecular mechanisms underlying IVM-mediated suppression of tumor growth have not been clearly determined. Therefore, the purpose of this study was to assess the anti-tumor effects of IVM on glioma cells and to explore the potential molecular mechanisms *in vitro* and *in vivo*.

Materials and Methods

Chemicals and Reagents

Ivermectin (IVM) was purchased from Sigma-Aldrich USA (European pharmacopoeia reference standard), and purity > 95%. MTT [3-(4, 5-dimethylthiazol-2-yl)-2, 5-diphenyl tetrazolium bromide] was purchased from Biotopped, purity > 95%. New-fetal bovine serum (NBS) was provided by Zhejiang Dayhang Biological Technology Co. Ltd (Hangzhou, China). Antibodies used in this study were against Bax (CST, #2774, USA), Bcl-2 (CST, #3498, USA), Cytochrome C (CST, #11940, USA), CDK2 (CST, #2546, USA), CDK4 (CST, #12790, USA), CDK6 (CST, #13331, USA), Cleaved caspase-3 (Bioss, bs-0081R, China), Cleaved caspase-9 (Bioss, bs-0049R, China), Cyclin D1 (CST, #2922, USA), Cyclin E (SRP5345, Sigma, USA), Ki67 (CST, #9129, USA), β-actin (A1978, Sigma, USA), Goat anti-Rabbit lgG (H+L)-HRP (Sungene, LK2001, China) and Goat anti-Mouse lgG (H+L)-HRP (ZSGB, ZB-2305, China).

Cell culture

Rat C6 glioma cells and human U251 glioma cells were obtained from The First Affiliated Hospital of

Harbin Medical University. Cells were cultured in Dulbecco's minimal essential medium (DMEM; HyClone, USA) supplemented with 10% New-fetal bovine serum (NBS) in a humidified incubator at 37°C under 5% CO_2 atmosphere. Cells were grown to 65%-75% confluency and treated under various conditions as indicated.

Cell viability assay

Cell viability was performed by MTT assay according to the manufacturer's instructions. C6 (8.0×10^3 cells/well), U251 (1.0×10^4 cells/well) and SVG p12 cells were seeded into 96-well plates overnight and treated with various concentrations of IVM for 24, 48 and 72 h at 37 °C, respectively. Cells were then incubated with MTT (5 mg/ml) for another 4 h at 37 °C. After the medium was carefully removed, 150 μL of dimethyl sulfoxide (DMSO; Sigma, USA) was added and agitated to dissolve the formazan crystals. Absorbance was measured at 490 nm on an enzyme-linked immunosorbent assay reader (HUADONG-Y, China). For relative quantification, the value of absorbance in each group was normalized to that in the control group.

Colony formation assay

To analyze the sensitivity of the cells to dopamine, we performed a colony formation assay *in vitro*. Briefly, C6 (3.0×10^2 cells/well) and U251 (4.0×10^2 cells/well) cells were seeded in 6-well plates for 24 h then treated with various concentrations of IVM (0, 5, 10 and 15 μmol/L). The cultures were maintained at 37°C in a 5% CO_2 incubator for 10 days, which allowed the viable cells to grow into macroscopic colonies. Then, the medium was removed, and the colonies were counted after being stained with 0.1% crystal violet (Sigma, USA). The number of colonies was counted under microscope. Quantification of colony formation was also performed using ImageJ software.

Cell apoptosis analysis

Annexin V-FITC detection is an effective method to distinguish apoptotic cells from normal cells by using Annexin V-FITC Apoptosis Detection Kit (Beyotime biotechnology, C1063). C6 (2.5×10^5 cells/well) and U251 (3.0×10^5 cells/well) cells were seeded in 6-well plates and treated with various concentrations of IVM (0, 5, 10, 15 μmol/L) for 48 h, cell suspensions were collected, then suspended in 195 μL of Annexin V binding buffer, 5 μL of Annexin V-FITC and 10 μL of PI were added, and the mixture was incubated for 20 mins at room temperature in the dark. The samples were analyzed immediately by flow cytometery (BD, Ariall, USA). The results were quantified using the Cell Quest software (BD Biosciences, USA), and Q2 plus Q4 area was calculated as the apoptosis ratio.

Cell cycle analysis

Apoptosis and cell cycle analyses of C6 and U251 cells were determined according to the cellular DNA content of the cell cycle, a method that is more reliable and full-scale. In this experiment, C6 and U251 cells were seeded in 6-well plates and cultured for 6 h, then incubated again with the medium in the absence or presence of IVM (15 μmol/L), respectively. After incubation for 24h or 48 h, cells were washed twice with an excess volume of ice-cold PBS. Then the cell precipitation was collected and added with pre-cooling alcohol of 75%. After fixing for more than 4 hours at 4°C, staining was done with PI staining solution, followed by flow cytometry analysis of the samples. The DNA content of the cell cycle was analyzed by modFit software.

Measurement of caspase activities

This assay was performed by using spectrophotometric detection of a colored reporter molecule, p-nitroaniline (*p*NA), which was linked to the end of the caspase-specific substrate. C6 and U251 cells were seeded in incubation bottles and cultured for 6 h, then treated with different concentrations IVM (0, 5, 10, 15 μmol/L) for 48 h. The treated cells were collected and then incubated with the peptide

substrate Ac-DEVD- *p*NA (acetyl-Asp-Glu-Val-Asp *p*NA), Ac-LEHD *p*NA (acetyl-Leu-Glu-His-Asp pNA) in assay buffer for 2 h at 37°C. The release of *p*NA was monitored at 405 nm.

Transmission electron microscopy (TEM)

Transmission electron microscopy (TEM) was used to analyze morphological characteristics of apoptosis. C6 and U251 cells were seeded in incubation bottles for 48 h (15 μmol/L IVM), and the untreated cells served as a control group. Then the cells were harvested, washed and fixed overnight with 2.5% glutaraldehyde containing 1% tannic acid at 4°C. After washing, the cell pellets were embedded in epon araldite (Polybed 812; Polysciences, Warrington, PA). The ultrathin sections were observed with a JEM-100CX transmission electron microscope (H-7650, China) and representative images were photographed and analyzed.

Western blotting

Western blotting was used to detect the expression of cell cycle-related and apoptosis-associated proteins. Glioma cells were treated with various concentrations of testing compounds (0, 5, 10, 15 μmol/L) for 48 h, then lysed with RIPA buffer (Solarbio, China) to extract total protein, which was subjected to sodium dodecyl sulfate-polyacrylamide gel (SDS-PAGE). Apoptosis-associated proteins and cell cycle-related proteins were probed, including Bax, Bcl-2, Cytochrome-c, Cleaved caspase-3, Cleaved caspase-9, CDK2, CDK4, CDK6, Cyclin D1 and Cyclin E. β-actin was used as loading control. Horseradish peroxidase conjugated secondary antibodies were used in conjunction with MiniChemi Imager (SageCreation, Beijing, China) for visualization.

Animal models

The studies were approved by the The Harbin Veterinary Research Institute in China. 7-week-old female Balb/c nude mice (Beijing vitonlihua experimental animal technology co. LTD, Beijing, China)

were treated with U251 cells (2.0×10^6) via subcutaneous injection. After 10 days, 12 mice were assigned randomly into two groups receiving 0.1 mL saline or 20 mg/kg IVM/mouse/day, respectively. Saline or IVM were injected intraperitoneally into mice every day. The volume of tumors were measured every four days by using a vernier caliper and calculated as length (mm) × width^2 (mm^2) × 1/2. All mice were euthanized with ether anesthesia for analysis after four weeks. Tumor tissues were isolated and frozen in liquid nitrogen immediately.

Immunohistochemistry

After 4 weeks, the mice were sacrificed, and harvested tumors were embedded into paraffin (Citotest, China). 5 μm-thick sections were labeled with antibody Ki67, Cleaved caspase-3, Cleaved caspase-9 by HRP-conjugated secondary antibody using diaminobenzidine (DAB; Sigma, USA) reagents as substrate and then counterstained with hematoxylin (Sigma, USA). Negative control was performed by omitting primary antibodies. Under × 400 magnification, the samples were carried out by counting the number of positive cell nuclei in 30 random fields from randomly chosen tumor sections for each animal.

TUNEL assay

The terminal deoxynucleotidyl transferase-mediated dUTP nickend labeling (TUNEL), which detects fragmented DNA, was performed using an In Situ Cell Death Detection Kit to evaluate the apoptotic response of tumor tissues, Fluorescein (Roche Diagnostics, Mannheim, Germany). Briefly, after being deparaffinized and hydrated, slides were washed with PBS twice and incubated with proteinase K (20 μg/ml) for 25 min at 37 °C. After a second round of washes, slides were incubated with TUNEL reaction mixture prepared freshly for 1 h at 37 °C in a moist chamber. After being washed twice, the slides were observed under fluorescence microscopy.

Statistical analysis

All experiments were repeated at least three times, and all results were presented as the mean ± SEM. Analyses of significance were performed by one-way ANOVA with post-test using Graph Pad Prism package (V5.0). Moreover, quantitative analyses of images (including immuohistochemical staining, western blotting) were carrieed out with ImageJ Software (V2.0), with $P < 0.05$ considered to be statistically significant.

Results

IVM inhibited the proliferation of glioma cells *in vitro*

To confirm the anticancer effects of IVM on glioma cells, the MTT assay was conducted to assess the growth viability of C6, U251 cells and normal human astrocyte (SVG p12), respectively. As shown in Fig.1A, IVM treatment for 48 h dramatically decreased the cell viability of glioma cells in a dose-dependent manner compared with normal glioma cells, and notably IVM exhibited a lesser effect on normal normal human astrocyte. Furthermore, IC50 values indicated that IVM was a more potent cytotoxic reagent in glioma cells compared with that in normal cells (Table 1). Consistently, C6 and U251 cell clonogenic capacity were employed, we found that IVM significantly inhibited colony formation and induced significant decrease in the colony formation ratio (Fig. 1B and C). These results showed that IVM significantly inhibited the glioma cell proliferation and had little effect on normal human astrocyte growth.

Induced apoptosis of glioma cells by IVM

The effect on the induction of cell apoptosis on glioma cells was examined by flow cytometry (Fig. 2A). As illustrated in Fig. 2B, Annexin-V-FITC/PI double staining assay showed that treatment with different concentrations of IVM for 48 h increased the percentage of apoptotic cells from 4.10 ± 0.00%

to 30.77 ± 2.01% in C6 cells. IVM-treated U251 cells had an increased apoptotic cells ratio from 3.90 ± 0.00% to 58.40 ± 1.16%. Thus, IVM induced apoptosis of C6 and U251 cells in a dose-dependent manner compared with control group ($P < 0.001$).

Effects of IVM on inducing cell cycle arrest

To further confirm the proliferation effects of IVM on cell cycle arrest in C6 and U251 cells, the cell cycle distribution was detected by PI staining and flow cytometry (Fig. 3A). As shown in Fig. 3B and C, the G0/G1 phase in 48 h reflects an upward trend in the percentage of the C6 cells from 53.38 ± 2.13% to 65.90 ± 1.16%, and for U251 cells from 58.29 ± 1.16% to 72.26 ± 1.19%, which were statistically significant compared with the control group ($P < 0.01$). In addition, the S phase showed a decreasing trend from 39.06 ± 2.30% to 34.10 ± 1.16% for C6 cells, and from 35.10 ± 1.90% to 24.41 ± 1.29% for U251 cells, whereas, the G2/M phase changes from 8.88 ± 2.32% to 0.05 ± 0.05% for C6 cells, and from 7.27 ± 1.23% to 3.33 ± 0.47% for U251 cells. And, there are no obvious changes of 24 h treatment. Taken together, these data indicated that IVM stimulated cell cycle arrest in glioma cells.

Ultrastructural morphologic changes in the glioma cells

To further clarify the morphological characteristics of apoptosis induced by IVM, TEM was performed to detect the cells treated with 15 μmol/L IVM. As shown in Fig. 4A and E, untreated C6 and U251 cells showed no obvious changes, displaying a complete cytoplasm and organelles. Conversely, the treated cells presented typical apoptotic features: cell shrinkage, apoptotic chromatin condensation (Fig. 4B and F), pervacuolization of cytoplasm and formation of apoptotic bodies (Fig. 4C and G). Furthermore, numerous large autophagicvacuoles in the cytoplasm were observed (Fig. 4D and H), in which the vacuolar contents were degraded, evidence for the impact of IVM in the regulation of autophagic formation in glioma cells.

Effects of IVM on caspase-3 and caspase-9 activities

Caspases propagate apoptosis reacting to pro-apoptotic signal. Activated caspase-9 immediately initiated a caspase cascade including the downstream executioner caspase-3, resulting in cell apoptosis [22]. The IVM-treated glioma cells were investigated for the activation of caspase-3/-9 by using spectrophotometric detection. As shown in Fig. 5C, both the activation of caspase-3 and caspase-9 were augmented in a dose dependent manner after IVM treating. Our results suggested that the apoptosis caused by IVM was accommodated via the activated caspase-3/-9.

IVM modulated the expression of apoptosis-related and cell cycle-related proteins

In order to investigate the mechanism of IVM against C6 and U251 cells, the expression levels of apoptosis-associated and cell cycle-associated proteins were individually detected by using western blotting analysis (Fig. 5A). As shown in Fig. 5C, we found that the quantity expressions of Bax, Cytochrome-c, Cleaved caspase-3 and Cleaved caspase-9 were increased and that Bcl-2 was decreased in a dose-dependent fashion as expected, compared with their respective internal control, β-actin. Moreover, IVM down-regulated the expression of cell cycle proteins like Cyclin D1, Cyclin E, CDK2, CDK4, CDK6 and β-actin remained unchanged.

U251 xenograft growth was suppressed *in vivo* by IVM

To evaluate the effects of IVM on glioma cells growth *in vivo*, Balb/c nude mice were employed for engraftment of human U251 cells. As shown in Fig. 6A, macroscopically, the size of control tumors was much larger than that of IVM-treated tumors. Xenografts treated with IVM grew at a slower rate than those treated with saline (Fig. 6B). No significant difference in the weights of the mice was observed between the experimental groups after all measured days (Fig. 6C). Ki67 staining and TUNEL assay demonstrated more dead cells and the evident increase in apoptosis proportion in

IVM-treated tumor tissues. Immunohistochemistry also demonstrated the increase in IVM-treated tumor tissues that stained positively for Cleaved caspase-3 and caspase-9 (Fig. 6D and E). Moreover, the levels of Cleaved caspase-3 and Cleaved caspase-9 in tumor xenograft tissues were measured by western blotting (Fig 6F). As showed in Fig. 6G, the expression of Cleaved caspase-3 and Cleaved caspase-9 increased noticeably compared with control group.

Discussion and conclusions

Glioma is a complex neuroglial tumor involving dysregulation of many biological pathways at multiple levels. Thus, poor treatment of glioma under current therapeutic regiments has necessitated the development of novel therapeutic agents. First in our study, we utilized a broad-spectrum antiparasitic drug IVM to test its anticancer function in glioma cells. Our results indicated that IVM decreased the cell viability of glioma cells in a dose-dependent manner compared with untreated glioma cells. Second, we provided evidence that IVM was able to block cell cycle G0/G1 phase and changed the morphological characteristics of apoptosis with TEM. Third, we also confirmed that IVM induced apoptosis by up-regulating the expression of Bax, down-regulating Bcl-2, leading to Cytochrome-c release, increasing caspase-3 and caspase-9 activation, and down-regulating levels of CDK2, CDK4, CDK6, CyclinD1 and CyclinE. Finally, the results revealed that IVM suppresses U251 xenograft growth *in vivo*. These findings suggested that IVM probably represent a promising agent in the treatment of glioma.

Next, the MTT assay and colony formation assay were was used to verify whether IVM could be a therapeutic agent for glioma cells. Our results showed that IVM conspicuously inhibits proliferation of C6 and U251 cells in a time- and dose-dependent manner. Furthermore, IVM exhibited a lesser effect on normal human astrocyte growth. So our data indicated that IVM can be used to prevent the

proliferation of cancer cells at a low and safe concentration.

Apoptosis is an evolutionarily conserved essential process for development and tissue homeostasis. What's more, several evidences exist to prove that inducing apoptosis might be considered as the major mechanism for chemotherapeutic agents against human malignancies, which belongs to programmed cell death (PCD) and widely exists in physiological and pathological conditions [23, 24]. Our results demonstrated that IVM induced cell apoptosis in C6 and U251 cells. The underlying mechanism of IVM-induced apoptosis in glioma cells was assessed by western blotting. Previous studies have mentioned that apoptosis was induced by the mitochondria pathway that mediated by the Bcl-2 family proteins [25-27]. It is well known that the members of the Bcl-2 family, including pro-apoptosis protein Bax and anti-apoptotic protein Bcl-2 are a pair of important regulating factors of apoptosis [28-31]. In the present study, IVM inhibited Bcl-2 expression and induced Bax expression. A high ratio of Bax to Bcl-2 can cause the release of Cytochrome-c. In addition, in the cytosol, Cytochrome-c resulted in the activation of caspase-3 and caspase-9. And the activated caspase-9 was cleaved and thereby induced the activation of other caspases, such as caspase-3, which in turn may influence mitochondrial function, and subsequently contributed to apoptotic cell death. These results showed that Bcl-2 acts primarily at the level of mitochondria to prevent this release. We considered that IVM induced cell death signaling may focus on the mitochondria-dependent pathway in glioma cells. However, it could not be excluded that the possibility of IVM-induced apoptosis results from the extrinsic pathway.

Cell cycle regulation is an important target of anti-proliferation in cancer treatment. The cell cycle progression from the G1 to S phase is related to the regulation of Cyclin-dependent kinases (CDKs) and cyclin complexes [32, 33]. In this study, the result revealed that the percentage of cells in G0/G1

phase showed an upward tendency and a striking decrease at S phase with the increase of IVM concentration. It is also telling that exposure to IVM induced G0/G1 cell cycle arrest and apoptosis which inhibited the growth of C6 or U251 glioma cells. To reveal the mechanism behind these changes, we investigated the specific cell cycle regulators of G0/G1 phase. Our western blotting analysis demonstrated that the level of CDK2, CDK4, CDK6, Cyclin D1 and Cyclin E proteins in the cells treated with IVM was significantly down-regulated in a dose-dependent manner compared with the control group. Additionally, some similar varying tendency in the mRNA level of these genes was observed on C6 and U251 cells. Additionally, Cyclin-CDK heterodimers played an important role in regulating the progression of cells through the G1 phase of cell cycle and initiation of DNA replication [34]. Hence, these all data manifested that block of G0/G1 transition might be one mechanism responsible for the noticeable apoptotic rate increase of glioma cells exposed to IVM, which induced cell arrest partly by down-regulating CDK2, CDK4, CDK6, Cyclin D1 and Cyclin E.

Meanwhile, the treatment of C6 and U251 cells presented the hallmarks of apoptosis by TEM including chromatin condensation and clustering along the nuclei membrane. These obvious characteristics manifested that IVM could induce glioma cell apoptosis. Future work is needed to analyze the mechanism of autophagy and the relationship with apoptosis induced in glioma cells by IVM.

Furthermore, the experiments *in vivo* were conducted according to the report that treatment of breast cancer bearing nude mice with IVM resulted in remarkable inhibition of the tumor growth without overall gross toxicity [35]. In our animal study, U251 cells was selected not merely because it belongs to human, but IVM could more significantly inhibit the proliferation of U251 cell *in vitro*. So in a follow-up experiment, it was found that the intraperitoneal injection of IVM at doses of 20 mg/kg

prominently inhibited the growth of glioma cells *in vivo*. Western blotting and immunohistochemistry analysis confirmed the increase in TUNEL, Ki67, Cleaved caspase-3, and Cleaved caspase-9 following IVM treatment. These results indicated that IVM could induce the apoptosis of glioma cells *in vivo*, and the activation of caspase-3 and caspase-9 were one of the key molecular events leading to IVM-mediated apoptosis of glioma cell.

In conclusion, the present study demonstrated that IVM had an inhibitory effect on viability of glioma cells *in vitro* and *in vivo* by inducing apoptosis and cell cycle arrest. We propose that IVM might be a potent and promising agent to combat glioma.

Acknowledgments

We thank Saadia Khilji for assisting in the preparation of the manuscript. This work was supported by the National Natural Science Foundation of China (No. 81201723 and 81501050) and the "Young Talents" Project of Northeast Agricultural University (No. 14QC05), Natural Science Foundation of Heilongjiang Province (QC2014C104) and the Heilongjiang Postdoctoral Fund (No. LBH-Z13027).

Conflict of interest

There is no conflict of interest.

References

1. Gao, J.H., et al., *Liposome encapsulated of temozolomide for the treatment of glioma tumor: Preparation, characterization and evaluation*. Drug Discoveries & Therapeutics, 2015. 9(3): p. 205-12.

2. Shen, X., et al., *EVA1A inhibits GBM Cell proliferation by inducing autophagy and apoptosis*. Experimental Cell Research, 2017. 352(1): p. 130-8.

3. Furnari, F.B., et al., *Malignant astrocytic glioma: genetics, biology, and paths to treatment*. Genes and Development, 2007. 21(21): p. 2683-10.

4. Dhandapani, K.M., V.B. Mahesh, and D.W. Brann, *Curcumin suppresses growth and chemoresistance of human glioblastoma cells via AP-1 and NFκB transcription factors*. Journal of Neurochemistry, 2007. 102(2): p. 522-38.

5. Anand, P., et al., *Bioavailability of curcumin: problems and promises*. Molecular Pharmaceutics, 2007. 4(6): p. 807-18.

6. Mason, W.P, and J.G. Cairncross, *Drug insight: temozolomide as a treatment for malignant glioma: impact of a recent trial*. Nature Reviews Neurology, 2005. 1(2): p. 88-95.

7. Newlands, E.S., et al., *Temozolomide: A review of its discovery, chemical properties, pre-clinical development and clinical trials*. Cancer Treat Rev. 1997. 23: p. 35-61.

8. Gilbert, M.R., et al., *Dosedense temozolomide for newly diagnosed glioblastoma: a randomized phase III clinical trial*. J. Clin. Oncol, 2013. 31: p. 4085-91.

9. Lan Y.L., et. al., *The potential roles of dopamine in malignant glioma*. Acta Neurol Belg, 2017. 117(3): p. 613-21.

10. Korystov, Y.N., N.V. Ermakova, and L.N. Sterlina, *Avermectins inhibit multidrug resistance of tumor cells*. European Journal of Pharmacology, 2004. 493(3): p. 57-64.

11. Mani, T., et al., *Interaction of macrocyclic lactones with a Dirofilaria immitis P-glycoprotein*, International Journal for Parasitology, 2016. 46(10): p. 631-40.

12. Egerton, J.R., et al., *Avermectins, new family of potent anthelmintic agents: efficacy of the B1a component*, Antimicrobial Agent & Chemotherapy, 1979. 15(3): p. 372-78.

13. González Canga, A., et al., *A review of the pharmacological interactions of ivermectin in several animal species*, Curr Drug Metab, 2009. 10(4): p.359-68.

14. Drinyaev, V.A., et al., *Antitumor effect of avermectins*, European Journal of Pharmacology, 2004. 501(1-3): p. 19-23.

15. Hashimoto, H., et al., *Ivermectin inactivates the kinase PAK1 and blocks the PAK1-dependent growth of human ovarian cancer and NF2 tumor cell lines*, Drug Discoveries & Therapeutics, 2009. 3(6): p. 243-6.

16. Sharmeen, S., et al.,*The antiparasitic agent ivermectin induces chloride-dependent membrane hyperpolarization and cell death in leukemia cells*. Blood, 2010. 116(18): p. 3593-603.

17. Melotti, A., et al., *The river blindness drug Ivermectin and related macrocyclic lactones inhibit WNT-TCF pathway responses in human cancer*. EMBO Mol Med, 2014. 6(10): p. 1263-78.

18. Dou, Q.H., et al., *Ivermectin Induces Cytostatic Autophagy by Blocking the PAK1/Akt Axis in Breast Cancer*. Cancer Res, 2016. 76(15): p. 4457–69.

19. Gao, A.L., et al., *Reversal of P-glycoprotein mediated multidrug resistance in vitro by doramectin and nemadectin*. Journal of Pharmacy & Pharmacology, 2010. 62(3): p. 393-99.

20. Liu, Y., et al., *Anthelmintic drug ivermectin inhibits angiogenesis, growth and survival of glioblastoma through inducing mitochondrial dysfunction and oxidative stress*. Biochemical & Biophysical Research Communications, 2016. 480(3): p. 415-21.

21. Yin, J., et al., *DEAD-box RNA helicase DDX23 modulates glioma malignancy via elevating miR-21 biogenesis*. Brain, 2015. 138(9): p. 2553-70.

22. Wu, H.J., et al., *Caspases: A Molecular Switch Node in the Crosstalk between Autophagy and Apoptosis*. Int J Biol Sci, 2014. 10(9): p. 1072-1083.

23. Han, Y.T., et al., *Physcion inhibits the metastatic potential of human colorectal cancer SW620 cells in vitro by suppressing the transcription factor SOX2*. Acta Pharmacologica Sinica. 2016 37(2): p. 264-75.

24. Zimmermann, K.C., C. Bonzon, and D.R. Green, *The machinery of programmed cell death*. Pharmacology Therapeutics, 2001. 92(1): p. 57-70.

25. Levine, B, and G. Kroemer, *Autophagy in the pathogenesis of disease*. Cell, 2008. 132(1): p. 27-42.

26. Jin, S, and E. White, *Role of autophagy in cancer: management of metabolic stress*. Autophagy, 2007. 3(1): p. 28-31.

27. Zhao, Y., et al., *Berbamine inhibited the growth of prostate cancer cells in vivo and in vitro via triggering intrinsic pathway of apoptosis*. Prostate Cancer and Prostatic Diseases. 2016. 19(4): p. 358-66.

28. Gustafsson, A.B, and R.A. Gottlieb, *Bcl-2 family members and apoptosis, taken to heart*. Am J Physiol Cell Physiol, 2007. 292(1): p. C45-51.

29. Youle, R.J., and A. Strasser, *The Bcl-2 protein family. Opposing activities that mediate cell death*. Nature Reviews Molecular Cell Biology, 2008. 9(1): p. 47-59.

30. Zhu, Y., et al., *The cytotoxic effect of β-elemene against malignant glioma is enhanced by base-excision repair inhibitor methoxyamine*. Journal of Neuro-Oncology, 2013. 113(3): p. 375-84.

31. Du, X.X., et al., *Initiation of apoptosis, cell cycle arrest and autophagy of esophageal cancer cells by dihydroartemisinin*. Biomedicine &Pharmacotherapy, 2013. 67(5): p. 417-24.

32. Lin, C.J., et al., *Preclinical effects of honokiol on treating glioblastoma multiforme via G1 phase arrest and cell apoptosis*. Phytomedicine. 2016. 23(5): p. 517-27.

33. Jung,Y.S., Y.J. Qian, and X.B. Chen, *Examination of the expanding pathways for the regulation of p21 expression and activity*. Cell Signal, 2010. 22(7): p. 1003-12.

34. John, P.C.L., M. Mews, and R. Moore, *Cyclin/Cdk complexes: their involvement in cell cycle progression and mitotic division*. Protoplasma, 2001. 216 (3-4): p. 119-42.

35. Gao, A.L., et al., *Reversal effects of doramectin on modulating resistance in MCF-7/adr cells in vitro*, Chinese Journal of Hospital Pharmacy. 2014. 34(4): p. 266-9.

Figure Legends

Figure1 IVM inhibited the cell proliferation *in vitro*. A: IVM inhibted the growth in glioma cells. Cell viability was measured by MTT assay in C6, U251 and SVG p12 cells, which incubated in the absence or presence of IVM at different concentrations for 24 h, 48 h and 72 h. B: IVM suppressed colony formation in glioma cells. Cells were cultured in the indicated concentrations of IVM for 10 days. C: Graphs represent the number of colonies.The statistical data were shown as mean ± SEM. $^{*}P < 0.05$, $^{**}P < 0.01$ vs. IVM 0 μmol/L.

Figure 2 The effect of IVM on apoptosis induction of C6 and U251 cells treated with different concentrations of IVM (0, 5, 10 and 15 μmol/L) for 48 h. A: Flow cytometry plots after 48 h for C6 and U251 cell populations labeled for apoptotic cells. B: The percentage of apoptotic cell population. IVM induced a significant apoptosis of C6 and U251 cells in a dose-dependent manner. The statistical data were shown as mean ± SEM. $^{**}P < 0.01$, $^{***}P < 0.001$ vs. IVM 0 μmol/L.

Figure 3 The effect of IVM on cell cycle progression of C6 and U251 cells treated with various concentrations of IVM (0, 15 μmol/L) for 24 h or 48 h. A: Representative histograms for changes in the cell cycle for C6 and U251 cells. B and C: Graphs represent the percentage of cells cycle distribution in the G0/G1, S and G2/M phases in C6 and U251 cells. The statistical data were shown as mean ± SEM. $^{*}P < 0.05$, $^{**}P < 0.01$ vs. IVM 0 μmol/L.

Figure 4 The morphological changes of C6 and U251 cells followed by TEM observation. A and E: Control cells without IVM. B-D, F-H: Cells treated with IVM (15 μmol/L) for 48 h. B and F: Typical apoptotic changes such as chromatin condensation, nuclear fragmentation, and apoptotic bodies are indicated with black arrows. C and G: Cytoplasmic and mitochondrial hypervacuolization are indicated with white triangles. D and H: Abundant autophagic vacuoles were observed after treatment with IVM,

autolysosomes (black triangle) are single-membrane structures containing degraded cellular contents. Scale bar, 1 μm.

Figure 5 Representative images and quantitative protein levels of C6 and U251 cells. A and B: C6 and U251 cells were treated with IVM for 48 h and then subjected western analysis for related apoptosis proteins of Bax, Bcl-2, Cytochrome-c, Cleaved caspase-3 and Cleaved caspase-9 and the cell cycle regulatory proteins of CDK2, CDK4, CDK6, Cyclin D1 and Cyclin E. C: Effect of IVM on caspase-3 and caspase-9 activities**.** Relative amounts of protein data are presented as mean ± SEM. $^{*}P < 0.05$, $^{**}P < 0.01$, $^{***}P < 0.001$ vs. IVM 0 μmol/L.

Figure 6 IVM suppressed U251 xenograft growth *in vivo*. Nude mice with U251 subcutaneous tumor xenografts were treated with saline or 20 mg/kg IVM every day by peritoneal injection for 3 weeks. The tumors were isolated (A) and volumes were measured (B). C: Charting of mice weight with time. D: Representative immunohistochemistry images of TUNEL, Ki67, Cleaved caspase-3 and Cleaved caspase-9 of U251 xenograft tissues from vehicle or IVM-treated mice. E: Quantitative analysis of Ki-67, Cleaved caspase-3 and caspase-9-positive cells in xenograft tissues of different groups. F: The expression levels of Cleaved caspase-3 and caspase-9 in tumor xenograft tissues with western blotting. G: Relative amount of indicated proteins are shown. The statistical data were shown as mean ± SEM. $*P < 0.05$; $**P < 0.01$; $***P < 0.001$ vs. IVM 0 μmol/L.

Table 1. Median inhibitory concentration (IC50) of IVM on the viability of glioma cells

	IC50 (μmol/L)		
	24 h	48 h	72 h
C6	25.35 ± 2.20	15.93 ± 1.39	10.38 ± 0.90
U251	21.40 ± 2.15	13.61 ± 0.99	6.73 ± 1.02
SVG P12	75.90 ± 2.87	53.74 ± 1.60	27.92 ± 1.57

Data are presented as the mean ± SEM; IC50, concentration required for 50% inhibition.

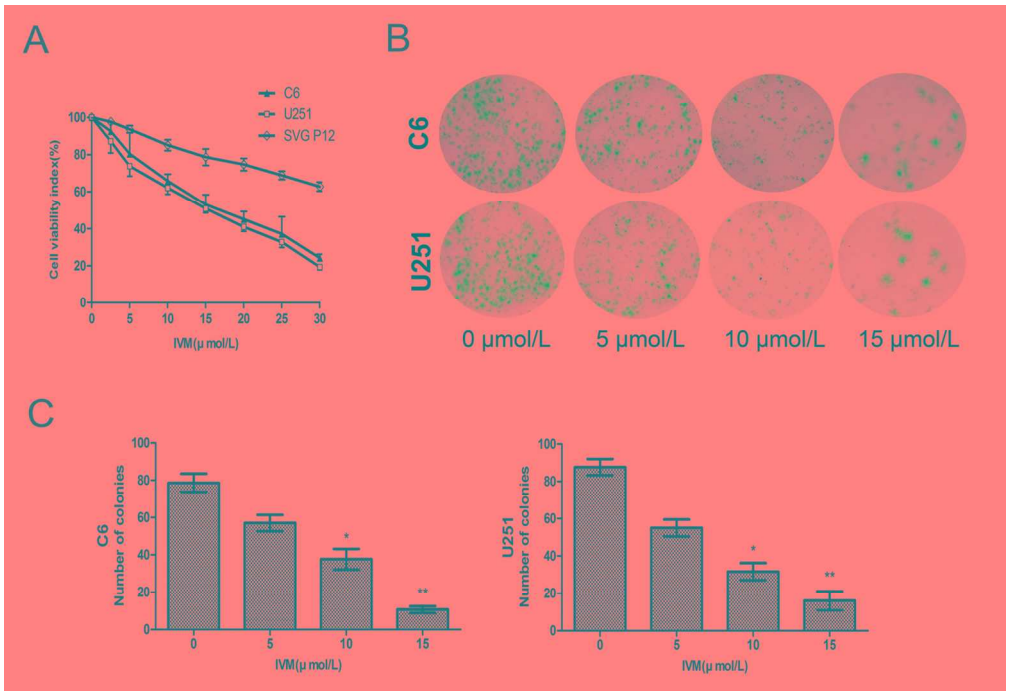

Figure1 IVM inhibited the cell proliferation in vitro.

146x100mm (300 x 300 DPI)

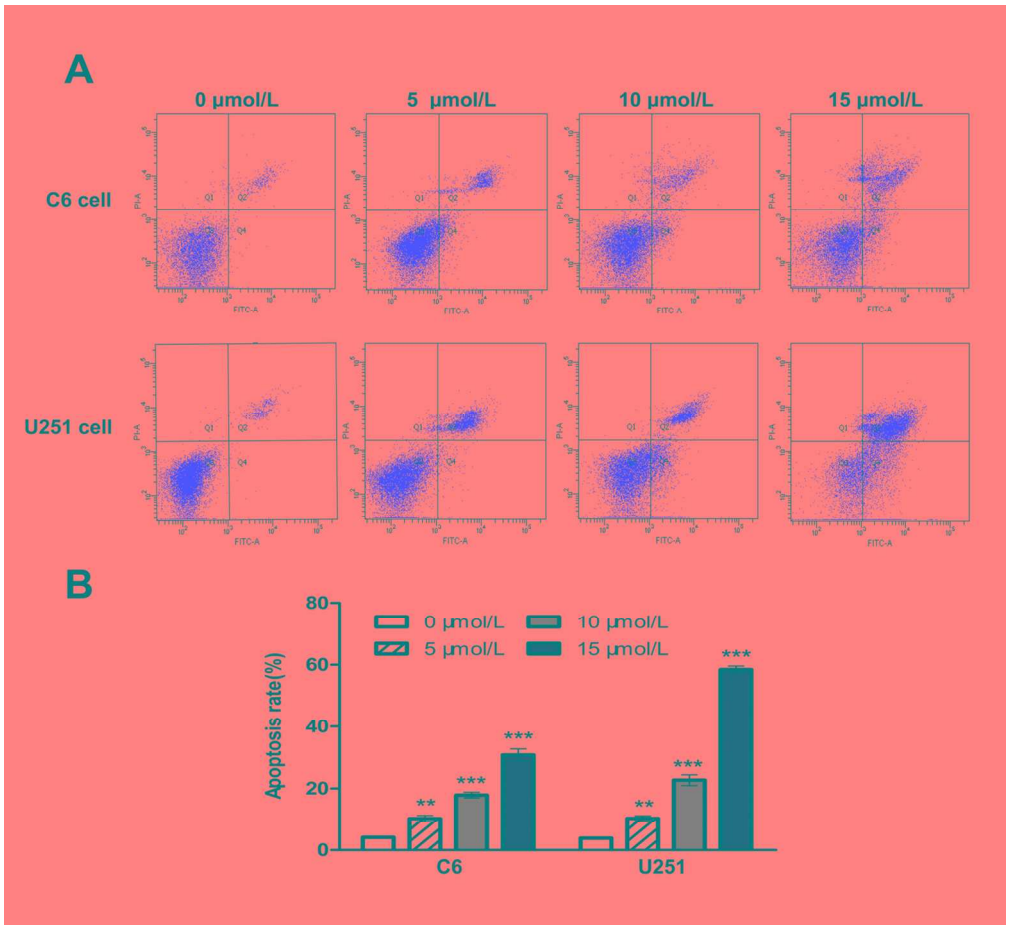

Figure 2 The effect of IVM on apoptosis induction of C6 and U251 cells treated with different concentrations of IVM (0, 5, 10 and 15 μmol/L) for 48 h.

155x143mm (300 x 300 DPI)

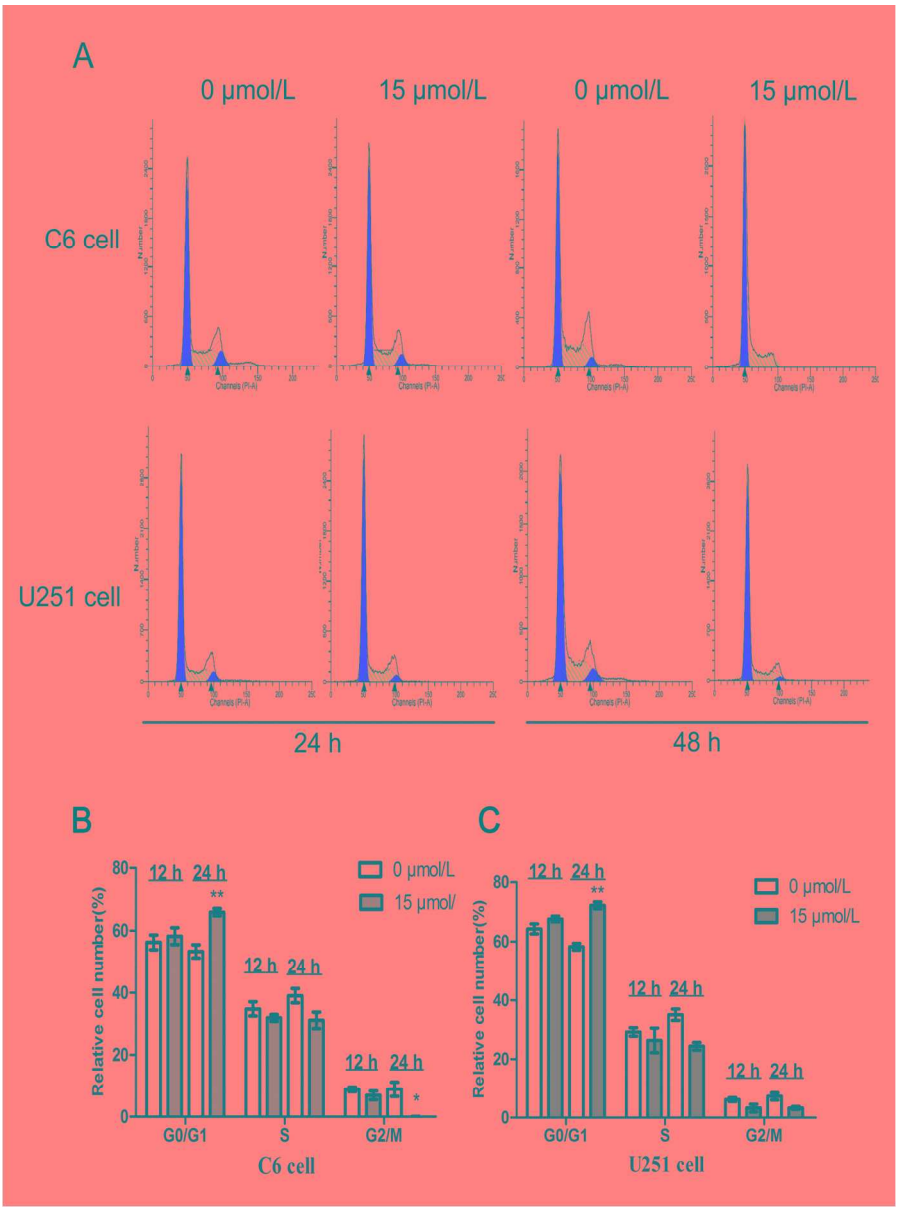

Figure 3 The effect of IVM on cell cycle progression of C6 and U251 cells treated with various concentrations of IVM (0, 15 μmol/L) for 24 h or 48 h.

234x314mm (300 x 300 DPI)

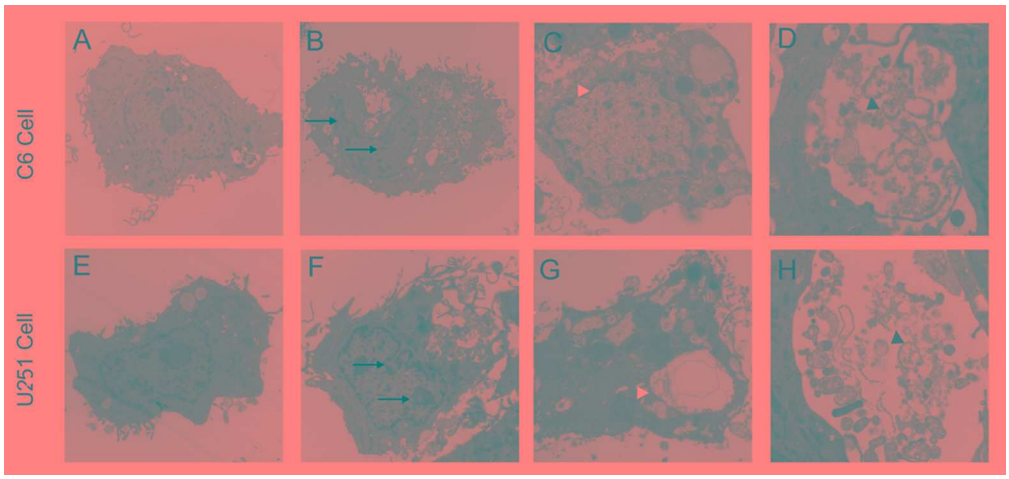

Figure 4 The morphological changes of C6 and U251 cells followed by TEM observation.

103x48mm (300 x 300 DPI)

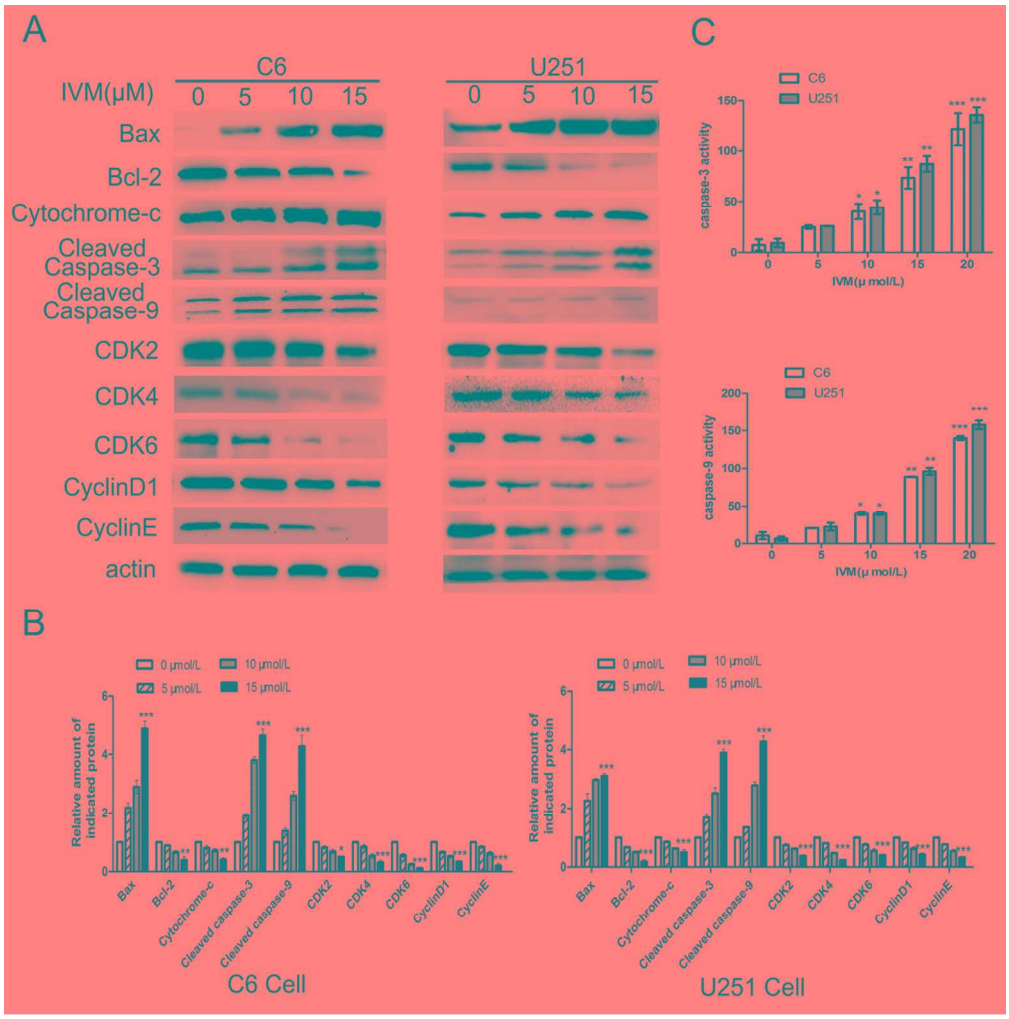

Figure 5 Representative images and quantitative protein levels of C6 and U251 cells.

171x172mm (300 x 300 DPI)

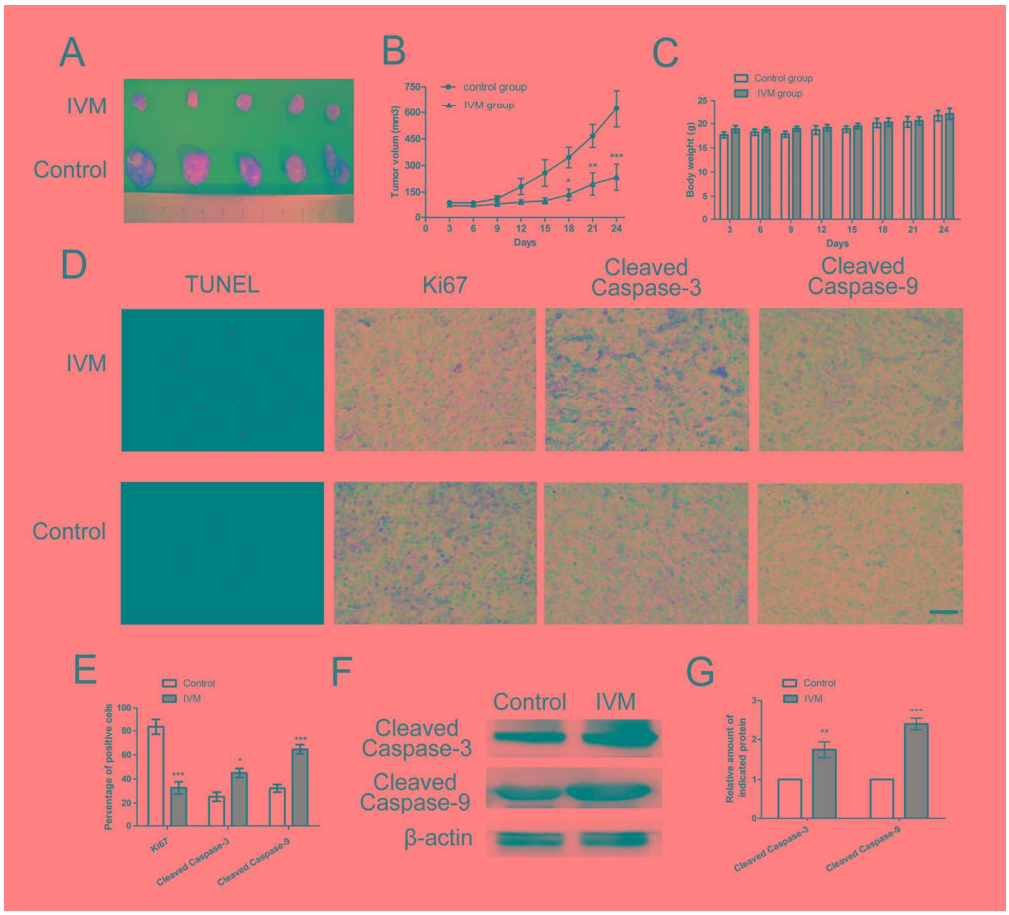

Figure 6 IVM suppressed U251 xenograft growth in vivo. Nude mice with U251 subcutaneous tumor xenografts were treated with saline or 20 mg/kg IVM every day by peritoneal injection for 3 weeks.

189x171mm (300 x 300 DPI)